Molecular Neurobiology (2022) 59:731–747
https://doi.org/10.1007/s12035-021-02600-w

Generation and Release of Neurogranin, Vimentin, and MBP Proteolytic Peptides, Following Traumatic Brain Injury

George Anis Sarkis[1,2,3,4] · Nicholas Lees-Gayed[4] · Joseph Banoub[5,6] · Susan E. Abbatielo[7] · Claudia Robertson[8] · William E. Haskins[9] · Richard A. Yost[2,10] · Kevin K. W. Wang[1,2,3,11]

Received: 24 June 2021 / Accepted: 12 October 2021 / Published online: 11 November 2021

Abstract

Traumatic brain injury (TBI) is a major neurological disorder without FDA-approved therapies. In this study, we have examined the concept that TBI might trigger global brain proteolysis in the acute post-injury phase. Thus, we conducted a systemic proteolytic peptidomics analysis using acute cerebrospinal fluid (CSF) samples from TBI patients and normal control samples. We employed ultrafiltration-based low molecular weight (LMW; < 10 kDa) peptide enrichment, coupled with nano-reversed-phase liquid chromatography/tandem mass spectrometry analysis, followed with orthogonal quantitative immunoblotting-based protein degradation analysis. We indeed identified novel patterns of injury-dependent proteolytic peptides derived from neuronal components (pre- and post-synaptic terminal, dendrites, axons), extracellular matrix, oligodendrocytes, microglial cells, and astrocytes. Among these, post-synaptic protein neurogranin was identified for the first time converted to neurogranin peptides including neurogranin peptide (aa 16–64) that is phosphorylated at Ser-36/48 (P-NG-fragment) in acute human TBI CSF samples vs. normal control with a receiver operating characteristic area under the curve of 0.957. We also identified detailed processing of astroglia protein (vimentin) and oligodendrocyte protein (MBP and Golli-MBP) to protein breakdown products (BDPs) and/or LMW proteolytic peptides after TBI. In addition, using MS/MS selected reaction monitoring method, two C-terminally released MBP peptides TQDENPVVHFF and TQDENPVVHF were found to be elevated in acute and subacute TBI CSF samples as compared to their normal control counterparts. These findings imply that future therapeutic strategies might be placed on the suppression of brain proteolysis as a target. The endogenous proteolytic peptides discovered in human TBI biofluid could represent useful diagnostic and monitoring tools for TBI.

Keywords TBI · Biomarker · NRGN · Vim · MBP · Peptidomics

✉ George Anis Sarkis
gasarkis@mit.edu; georgemr@ufl.edu;
georgekrekorian@gmail.com

✉ Kevin K. W. Wang
kwang@ufl.edu

[1] Program for Neurotrauma, Neuroproteomics & Biomarkers Research, Departmentof Emergency Medicine, University of Florida, Gainesville, FL 32611, USA

[2] Department of Chemistry, University of Florida, Gainesville, FL 32611, USA

[3] Department of Psychiatry, University of Florida, Gainesville, FL 32611, USA

[4] Department of Chemistry, Faculty of Science, Alexandria University, Ibrahimia, PO Box 426, Alexandria 21321, Egypt

[5] Fisheries and Oceans Canada, Northwest Atlantic Fisheries Centre, ScienceBranch, St. John's Newfoundland, Canada

[6] Biochemistry Department, Memorial University of Newfoundland, St. John's, NF, Canada

[7] The Barnett Institute of Chemical and Biological Analysis, Northeastern University, 360 Huntington Ave, Boston, MA 02115, USA

[8] Department of Neurosurgery, Baylor College of Medicine, Houston, TX, USA

[9] Gryphon Bio, Inc, 611 Gateway Blvd. Suite 120 #253, South San Francisco, CA 94080, USA

[10] Southeast Center for Integrated Metabolomics, University of Florida, Gainesville, FL 32610, USA

[11] Brain Rehabilitation Research Center, Malcom Randall Veterans Affairs Medical Center, 1601 SW Archer Rd, Gainesville, FL 32608, USA

Introduction

Traumatic brain injury (TBI), which is also known as a silent epidemic and no FDA-approved therapeutic interventions[1, 2], is defined as brain neurotrauma caused by a mechanical force that is applied to the head. In the USA, there are approximately 2.1 million incidents of TBI annually [3–5]. Besides, the Center for Disease Control and Preventions (CDC) reported that approximately 5.3 million Americans live with the effects of TBI [6]. About half of the Americans who experience TBI each year incur at least some short-term disability. The Armed Forces Health Surveillance Center has reported that almost 300,000 service members sustained TBI between 2000 and 2014 [7]. The severity of TBI ranges from severe and penetrating to mild or "concussion." TBI can also be classified by the Glasgow Coma Scale score as severe (GCS 3–8); moderate (GCS 9–12); and mild (GCS 13–15) [6]. Mild TBI accounts for over 85% of all cases [8]. Yet, to date, TBI remains a major neurological disorder without any FDA-approved treatments.

The physical impact of TBI and the subsequent triggering of glutamate excitotoxicity and the opening of calcium and sodium channels are thought to induce calcium and other ion influx and cellular homeostasis imbalance in the affected brain cells [9, 10]. Protease is one class of cellular enzymes in the brain found to be dysregulated after TBI [11, 12]. For example, the calcium-activated calpain has been strongly tied to axonal protein breakdown (e.g., αII-spectrin, neurofilament protein NF-H, NF-M) [11, 13–15] during the initial, acute pro-necrotic cell injury. In parallel, pro-apoptosis caspases are activated in neurons, also attacking αII-spectrin and other protein substrates in a delayed fashion [13]. Astroglial GFAP protein is a known substrate for calpain [16, 17] and caspase-6 [18]. Similarly, we previously detailed that myelin component myelin basic protein (MBP) isoforms are highly vulnerable to degradation by calpain and other proteases following experimental TBI in rats [19, 20]. Other protease classes also activated in neurotrauma and other neuro injury conditions are matrix metalloproteinases (MMPs) and lysosome-originated cathepsins (B, D) [21–24]. Although not related to TBI, transmembrane protein shedding also occurs in normal and pathological processes. For example, MMPs (ADAM10 and ADAM17) work as α-secretases to cleave the amyloid precursor protein (APP) at the juxtamembrane site and release sAPP extracellularly. The same MMPs also proteolytically release anti-aging protein Klotho (KL) from the cell surface. These cleaved forms of sAPP and KL are found in cerebrospinal fluid (CSF) and/or blood [25]. Similarly, neuronal activity can trigger the MMP-mediated cleavage of synaptic cell adhesion molecules (e.g., I-CAM-5 and neuroligin) [26]. These shed proteins can be bioactive.

While protein fragmentation is known to produce larger protein breakdown product (BDP) comparable in size to the intact protein (e.g., the 280 kDa αII-spectrin generates BDP of 150, 145, and 120 kDa, and the 50 kDa GFAP generates BDPs of 44–38 kDa) [17]. Yet, what is less appreciated is that proteolysis can often lead to the release or shedding of low molecular weight (LMW) peptides (often < 5 kDa). The "peptidome" in a healthy brain represents an array of bioactive neuropeptides and some levels of peptides were derived from non-specific, intact protein truncation at the N- and C-terminals [27, 28]. The concept of pathologic peptidome as a possible source of bioactive molecules or biomarkers has been proposed for neurodegenerative diseases, such as Alzheimer's disease and other human diseases [27, 29]. If there is an activation of multiple proteases following TBI, we propose that it should result in the generation of larger protein fragments or BDPs of a range of brain proteins, as well as shedding of LMW proteolytic peptides. We and others have studied protein breakdown products, such as αII-spectrin-spectrin, βII-spectrin, Tau, TDP-43, GFAP, and MBP, CRMP-2 [13, 16, 17, 19, 22, 30–32]. However, to the best of our knowledge, there are no systematic studies of proteolytic peptidome following TBI. Peptidomics study differs from the classic proteomic study, which requires the initial proteins to be in vitro pre-digested with trypsin protease into smaller LMW tryptic peptides to facilitate accurate mass and sequence determination. Yet in the peptidomics study described herein, as we are dealing with small peptide sizes (< 5–10 kDa), biosamples containing such peptides can be directly subjected to LC–MS/MS-based analysis without the extra step of tryptic digestion.

In this study, we examined the concept that TBI in human might trigger activation of intracellular and extracellular proteases such as calpains, caspases, cathepsins, and matrix metalloproteases resulting in global brain protein breakdown and release of proteolytic peptides. In our primary experiments, we use CSF samples from TBI and control subjects. Processed biosamples will be first subjected to ultrafiltration-based enrichment which will provide the LMW peptide fraction before global peptidomics analysis (with nano-LC-tandem spectrometry). In parallel, the high molecular weight (HMW) retentate fractions containing the intact proteins and their HMW BDPs were analyzed by immunoblotting analysis. We were capable to identify the proteolytic peptides released from three brain proteins, namely neuronal synaptic protein neurogranin, astrocyte cytoskeletal protein vimentin, and oligodendrocyte's MBP. Furthermore, the digestion of the purified protein with calpain and characterization of a larger protein fragment and proteolytic peptides was also conducted with verification data.

Materials and Methods

Human TBI and Control Cerebrospinal Fluid Procurement

The normal control samples CSF were purchased (Bioreclamation Co., USA). They were collected from healthy subjects using the lumbar puncture method by a qualified health professional. Archived de-identified CSF samples from a severe TBI study were collected from consenting adult subjects presenting to the emergency department of the Ben Taub General Hospital, Baylor College of Medicine (Houston, TX, USA). The study protocol was approved by the Baylor College of Medicine IRB, for subjects sustaining blunt trauma to the head with a Glasgow Coma Scale of 12 or less at 24 h (clinical trial registration NCT00313716; study title: "Effects of Erythropoietin on Cerebral Vascular Dysfunction and Anemia in Traumatic Brain Injury") [33]. CSF samples were collected with buretrol for up to 10 days or until an intra-ventriculostomy was no longer clinically indicated. Timed CSF samples (10 mL) with a total collection time not exceeding 1 h were diverted to 15-mL conical polypropylene centrifuge tubes (BD Falcon, USA) by a qualified and trained hospital employee according to the hospital's standard procedures. These CSF samples (5 to 10 mL) were then centrifuged at 4000 × g with a tabletop centrifuge at room temperature for 5 to 7 min to remove loose cells and debris. A volume of 1 mL aliquots of cleared CSF (supernatant) was pipetted into a 2-mL cryogenic tube, snap-frozen, and stored at − 80 °C in an ultra-low freezer until further use. For this study, timed CSF samples collected within 48 h of injury were used.

Ultrafiltration Method and Ultrafiltrate Processing for High-Resolution Orbitrap Mass Spectrometry

The ultrafiltration step is introduced to partition small peptides from higher molecular weight protein or protein fragments using an ultrafiltration unit with a molecular weight cutoff (MWCO) of 10 kDa membrane filter units (Sartorius Stedim Biotech, VS0102). The human CSF sample (250 µL) was loaded into the ultrafiltration cell and centrifuged at 4 °C for 5–20 min, 5000 × g [Eppendorf 5415R]. The 200 µL of the retentate was subject to separation and identification through Western blot analysis, while the 50 µL filtrate was concentrated using a speed vacuum (Thermo Scientific) to a volume of 10 µL. The ultrafiltrate samples (containing peptides) were separated by reversed-phase chromatography using a nanoflow liquid chromatography system (Dionex Ultimate 3000 RSLC; Thermo Scientific) interfaced with a hybrid ion trap-Orbitrap high-resolution tandem mass spectrometer (Velos-Pro; Thermo Scientific) operated in data-dependent acquisition (DDA) mode. Velos Pro Orbitrap is a hybrid mass spectrometer consisting of a dual cell linear ion trap and an Orbitrap mass analyzer that has an independent MS detector. Briefly, 1 µL of each sample was injected into a capillary column (C18 Onyx Monolithic, 0.10 × 150 mm Phenomenex) at a flow rate of 300 nL/min. Samples were electro-sprayed at 1.2 kV using a dynamic nanospray probe with fused silica non-coated emitters (20 µM ID with 10 µM ID tip PicoTip Emitter from New Objective). Chromatographic separation was carried out using 95 min linear gradients (mobile phase A: 0.1% formic acid in MS-grade water; mobile phase B: 0.1% formic acid in MS-grade acetonitrile), from 3% B to 35% B over 90 min, then increasing to 95% B over 5 min. MS/MS spectra were acquired using both collision-induced dissociation (CID) and higher-energy collisional dissociation (HCD) for the top 15 peaks in the survey 30,000 resolution MS scan. All MS/MS spectra were analyzed using Proteome Discoverer 2.2 (Thermo), SEQUEST HT (version: 2.2.0.388). Database search engines were set up to search with no enzyme UniProt-*Homo sapiens* (28,277 sequences and 17,749,896 residues) and FASTA file version 2019_06. The search was achieved using the average mass for matching the precursor with a fragment ion mass tolerance of 0.6 Da for the CID while 0.05 Da for the HCD and a precursor mass tolerance of 10 ppm. Carbamidomethylation of cysteine was selected as a static modification, while the oxidation of methionine was selected as a dynamic modification, using the output from SEQUEST HT. The peptides are validated within the database search results by using 1% for the strict FDR (false discovery rate), the search-dependent score (Xcorr > 2.0). Deviation of the measured mass from the theoretical mass of the peptide, in ppm (ΔM [ppm]), is set < 5 ppm for HCD and < 10 ppm for CID.

Gel Electrophoresis, Coomassie Blue Staining, and Immunoblotting

Ultrafiltration retentate samples (and unfiltered samples) are subjected to sodium dodecyl sulfate–polyacrylamide gel electrophoresis or SDS-PAGE. Twenty micrograms of protein from tissue lysate (20 µg protein), 100 ng of purified protein, or 10 µL of CSF retentate is mixed with SDS-containing sample buffer along with rainbow molecular weight marker full-range rainbow (RPN800E) and low-range rainbow (RPN755E, GE Healthcare, USA), and Novex Tris–glycine gel (18%, 1 mm × 10 well, or 10–20%, 1 mm × 12 well) was run on 200 V, for about 2 h. For purified protein samples, Coomassie Blue R-250 staining solution (0.1% CBB R250, 10% acetic acid, 40% methanol

in Milli-Q water) was used to visualize the protein bands, followed by destaining (10% acetic acid, 40% methanol).

For immunoblotting, the gel was placed in deionized water for 5 min and then in transfer buffer (25 mM Tris, 192 mM glycine, 20% methanol) for 5 min before electrotransfer to PVDF membrane on the iBlot Dry Blotting System (Carlsbad, CA, USA) at 20 V for 7 min. The PVDF was blocked with non-fat milk (5%) in Tris-buffered saline Tween (TBST) [20 mM, Tris pH 7.5, 15 mM NaCl 0.02% Tween 20] and probed with specific primary antibodies: neurogranin polyclonal; Upstate 07,425 or EMD AB5620; rabbit polyclonal or EMD Millipore ABN426; anti-vimentin (Abcam, Ab92547, rabbit polyclonal); anti-MBP (SMI99 MAb); custom MBP fragment epitope antibody (rabbit polyclonal); αII-spectrin Mab (BML-FG6090, ENZO Life Sciences); and β-actin (clone AC-15, A5441, Sigma) as 1:500 to 1:3000 in 5% skim milk in TBST overnight at 4 °C, followed by secondary goat anti-rabbit IgG AP conjugate (Fc specific) or goat anti-mouse IgG AP conjugate 69,266 [EMD Millipore, USA] for 2 h. Immunoreactive bands were then observed by adding 5-bromo-4-chloro-3-indolyl phosphate (BCIP) and nitro blue tetrazolium (NBT) [product code: 50–81-10], and the dried membrane was scanned with Expression 8836XL (Epson) and the UN-SCAN-IT software (version 6.1, Silk Scientific Corporation). Quantitative evaluation of the protein levels was performed with the computer-based densitometric NIH ImageJ (version 1.6) software.

Results

We have developed a novel and yet simple methodology to harness the enrichment and detection of TBI proteolytic peptidome in human CSF samples (Suppl. Figure 1). This novel methodology allowed the concurrent monitoring of the conversion of the parent proteins into HMW (high molecular weight) BDPs. Consequently, we utilized a system composed of a single-use ultrafiltration cell (300 µL capacity) fitted with a low MW cutoff (e.g., 10 K MWCO) membrane filter. Following this centrifugation-based separation, the obtained ultrafiltrate fraction contained the enriched native peptide pool that reflected and displayed a fingerprint marker for the injured brain only. The retentate fraction was enriched with intact proteins and their possible HMW BDPs (Suppl. Figure 1). For the ultrafiltration process, we chose a 10 K MWCO membrane to reduce the chances of losing the LMW peptides, which might have a secondary confirmation and thus might have difficulty passing through smaller filter pore sizes (e.g., 3 K MWCO).

Human TBI Cerebrospinal Fluid Proteolytic Peptidome

We have used the cerebrospinal fluid (CSF) samples from TBI and control subjects. The subject demographics and clinical characteristics are described in Table 1. The processed biosamples were first subjected to the ultrafiltration-based (10 K MWCO) enrichment of low molecular weight (LMW) peptide fraction before the global peptidomics tandem mass spectrometry analysis (using nano-LC-tandem mass spectrometry). In parallel, HMW retentate fractions (or unfiltered fraction) containing intact proteins and their HMW BDP's were subjected to complementary immunoblotting analysis for targeted protein integrity.

Using high-stringency selection criteria and filtering out those proteins also found in normal CSF, Table 2 lists proteins from which proteolytic peptides were exclusively identified from TBI CSF samples. The human TBI CSF ultrafiltrate proteolytic peptides originated from proteins found in many brain cell types and subcellular structures of neurons. Additionally they include proteins derived from neuron-axons (APBB1IP, CAMSAP1, CAMSAP3, NEFM, NEFL, SPTAN1, SPTBN1, SPTBN2, SPTBN4, GAP43); neuron-cell body (BASP1, SYNE1 (Nesprin-1), HTT); presynaptic terminal (SYN1, SYN3, SYNJ1, NRXN1); post-synaptic terminal (neurogranin (NRGN), CAMK2B, DLG4/PSD95); neuron-dendritic (MAP2, MAP6, STRN, TBB5); extracellular matrix [CSPG4, NCAN (CSPG3), brevican (CSPG7)]; oligodendrocyte (MBPA1, MBP, MYEF2, MYT1); astrocyte (ALDOC, GFAP, VIM); and also microglia/macrophage (MRC1) (Table 2). The representative proteolytic peptides identified from human TBI CSF ultrafiltrate samples are shown in Suppl. Table 2. Thus, our data revealed that specific proteins within major brain cell types (neurons, astroglia, and oligodendrocytes) and extracellular matrix are vulnerable to proteolytic attacks following TBI.

Human Brain Neurogranin, Vimentin, and Myelin Basic Protein Proteolytic Peptide and Breakdown Product Formation After TBI

To further study the patterns of the post-TBI proteolytic peptide formation, we performed an in-depth analysis of peptides derived from three brain proteins: neurogranin from neurons, vimentin predominantly from astrocytes, and myelin basic protein (MBP) isoforms from oligodendrocytes. NRGN is a small post-synaptic protein that participates in synaptic signaling between axon terminals in the brain. NRGN binds to calcium-bound calmodulin—which in turn activates the protein kinase C pathway [34]. We are consistently finding that the production of the proteolytic peptides were derived from the middle molecule of human TBI CSF patients. A cluster of peptides from residue 13–68

Table 1 Severe TBI and normal subject demographic and clinical characteristics

	Control ($N=29$)	TBI ($N=66$)
Age, years mean (SD)	41.6 (13.71)	40.41 (14.16)
Min–max	20–69	15–68
Male	20	57
Female	9	9
Ethnicity		
White, not Hispanic	15	32
Black, not Hispanic	11	16
Asian, not Hispanic	0	2
Hispanic	3	16
Mechanism of injury		
Motorcycle	n.a	34
Assault	n.a	9
Fall	n.a	9
Automobile	n.a	10
Auto-pedestrian	n.a	2
Sports	n.a	1
Bicycle	n.a	1
Severity—GCS-24 h (Glasgow Coma Scale)		
3	n.a	2
4	n.a	1
6	n.a	14
7	n.a	19
8	n.a	15
9	n.a	6
10	n.a	7
12	n.a	2
Cranial CT (Marshall Scale)		
D2—diffused injury II	n.a	25
D3—diffused injury III	n.a	24
D4—diffused injury IV	n.a	2
M1—evacuated mass lesion	n.a	14
M2—unevacuated mass lesion	n.a	1
Outcome—GOS (Glasgow Outcome Scale) at 6 months		
D = death	n.a	8
SD = severe disability	n.a	26
MD = moderate disability	n.a	19

Table 1 (continued)

	Control ($N=29$)		TBI ($N=66$)	
GR = good recovery	n.a		8	
LTF = loss to follow-up	n.a		5	

n.a. not available

was consistently identified. There are variations of their length—again suggesting alternative cleavages by the same protease (e.g., calpain) or action of multiple proteases (Fig. 1, Suppl. Fig. S2). For instance, peptide: ILDIPLDDPGANAAAAKIQAS(*)FRGHMARKKIKS(*)GERGRKGPGPGGPGGA (aa 16–64) is located within the center of human neurogranin (Suppl. Fig. S2). We also found that Ser-36 and 48 are a target for phosphorylation (*) in separate experiments (data not shown). Using label-free mass spectrometry based quantification of P-NRGN-BDP in human TBI CSF ($N=10$) vs. control ($N=10$) showed a significant difference between these groups (Fig. 1B). Furthermore, we used immunoblots to examine the levels of intact neurogranin and its major BDP (NRGN-BDP-7 K) in TBI CSF, on an immunoblotting analysis for NRGN, and probing it with an anti-neurogranin antibody, the intact neurogranin, which has a calculated size of 7.5 kDa, appears as a 15 kDa on the SDS-PAGE gel [35–37] instead of 7.5 kDa. We found that their median levels were significantly elevated in TBI CSF ($N=66$) within 24 h when compared to control CSF ($N=29$) (Fig. 1C). Lastly, receiver operator characteristic (ROC) curves of intact NRGN and NRGN-BDP were generated to compare control vs. TBI CSF. The ROC area under the curve (AUC) are 0.960 for intact NRGN ($p<0.0001$) and 0.999 for NRGN-BDP ($p<0.0001$) (Fig. 1D).

Vimentin is one of the major intermediate filament proteins that encode for the constituents of the cytoskeleton of many mammalian cells [38], found in the human brain regions such as the cerebellum, hippocampus, and entorhinal cortex. The levels of vimentin were found to increase in mechanically induced brain damage in mice as well as after TBI [39]. Vimentin (53.68 kDa), similar to GFAP, serves as an indicator of the presence of astrocyte activation (gliosis) [40]. We have identified two distinct clusters of proteolytic peptides in the ultrafiltrates of TBI CSF patients based on human vimentin (466 amino acids): N-terminal region (aa 1–74) and C-terminal region (aa 388–456), with a few minor internal peptides (Fig. 2, Suppl. Fig. S3). One such example is a proteolytic peptide, NVKMALDIEIATYRKLLEGEES(*)RIS(*)LPLPNFSSLNLRETNLDSLPL (aa 388–433), near the C-terminal (Suppl. Fig. S3). It contains two phosphorylation sites (*). Using label-free mass spectrometry based quantification of VIM N- and C-terminal peptides in human TBI CSF vs. control, TBI shows a significant difference between these groups for both peptides (Fig. 2A). In parallel, we also probed the human CSF and TBI CSF retentate on immunoblots with an anti-vimentin antibody; we observed three major VIM-related species: the intact vimentin (54 K), major VBDP-38 K, and a fainter VBDP-26 K (Fig. 2B). The VBDP-38 K likely represents a key fragment following clipping at both N- and C-terminals by endogenous protease(s). The median levels of intact VIM, VBDP-38 K, and VBDP-26 K were all significantly

Table 2 Selected human brain protein with proteolytic peptides identified in human TBI CSF ultrafiltrate by nLC-MS/MS. The data shown is a combined list of the brain-specific and enriched proteins with peptides uniquely found in human TBI CSF samples but not in normal control CSF samples. For representative peptides found for the listed proteins, see Suppl. Table 2

Accession number	Full protein name	Human gene name	Molecular weight (kDa)	Origin
Q96GW7	Brevican core protein (CSPG7)	BCAN	99.1	Extracell. matrix
P80723	Brain soluble acidic protein 1	BASP1	25	Neuron-cell body
Q5T5Y3	Calmodulin-regulated spectrin-associated protein 1	CAMSAP1	177.9	Neuron-axonal
Q9P1Y5	Calmodulin-regulated spectrin-associated protein 3	CAMSAP3	134.7	Neuron-axonal
Q13554-2	Calcium/calmodulin-dependent protein kinase II beta	CAMK2B	60.4	Post-synaptic term
Q6UVK1	Chondroitin sulfate proteoglycan 4	CSPG4	91.7	Extracell. matrix
P78352	Disks large homolog 4, PSD95	DLG4	80.5	Post-synaptic term
P09972	Fructose-bisphosphate aldolase C	ALDOC	39.4	Astrocyte
P17677	Growth associate protein (neuromodulin isoform 2/BASP2)	GAP43	26.1	Neuron-axonal
P14136	Glial fibrillary acidic protein	GFAP	49.8	Astrocyte
P42858	Huntingtin	HTT	347.1	Neuron-cell body
P22897	Macrophage mannose receptor 1 (MRC1, CD206)	MRC1	158.1	Microglia/macrophage
P11137	Microtubule-associated protein 2	MAP2	199.4	Neuron-dendritic
Q96JE9	Microtubule-associated protein 6	MAP6	86.5	Neuron-dendritic
P02686-3	Myelin basic protein, isoform 4 (21.5 K)	MBP	21.5	Oligodendrocyte
P02686-1	Golli-MBP, isoform 3 (myelin A1), HOG7	MBPA1	33.1	Oligodendrocyte
Q9P2K5	Myelin expression factor 2	MYEF2	64.1	Oligodendrocyte
Q01538	Myelin transcription factor 1	MYT1	125.1	Oligodendrocyte
O14594	Neurocan core protein (CSPG3)	NCAN	143	Extracell. matrix
Q92686	Neurogranin	NRGN	8.4	Post-synaptic term
Q8NF91	Nesprin-1 (nuclear envelope spectrin repeat protein-1)	SYNE1	1010.5	Neuron-cell body/nucleus
Q9ULB1	Neurexin-1 alpha	NRXN1	162.5	Pre-synaptic term
E7ESP9	Neurofilament medium polypeptide	NEFM	98.4	Neuron-axonal
P07196	Neurofilament light polypeptide	NEFL	59.7	Neuron-axonal
A6NG51	Spectrin alpha chain, nonerythrocytic 1	SPTAN1	284.8	Neuron-axonal
Q01082	Spectrin, beta, nonerythrocytic 1	SPTBN1	272.5	Neuron-axonal
O15020	Spectrin beta nonerythrocytic 2	SPTBN2	271.3	Neuron-axonal
Q9H254	Spectrin, beta, nonerythrocytic 4	SPTBN4	289	Neuron-axonal

Table 2 (continued)

Accession number	Full protein name	Human gene name	Molecular weight (kDa)	Origin
O43815	Striatin	STRN	86.1	Neuron-dendritic
P17600	Synapsin I	SYN1	74.1	Pre-synaptic term
O14994	Synapsin III	SYN3	63.3	Pre-synaptic term
C9JFZ1	Synaptojanin-1	SYNJ1	149.2	Pre-synaptic term
P07437	Tubulin beta 5	TBB5	49.6	Neuron-dendritic
P08670	Vimentin	VIM	53.7	Astrocyte

higher in TBI CSF retentate than their control counterparts (Fig. 2C).

Myelin basic proteins are key structural protein in oligodendrocytes in forming and stabilizing the myelin sheath around axonal fibers. Finally, we also profiled MBP proteolysis patterns in human TBI CSF patients. As anticipated, we observed strong proteolytic peptide signals in human TBI CSF (Fig. 3). The majority of these peptides clustered around residue N-terminal region: aa 11–24; center region: aa 105–118, 119–141; and C-terminal region aa: 165–178 (based on classic MBP-21 K isoform 3; P02686-3). We observed many peptides breaking off from this central region such as TQDENPVVHF (aa 107–116) and TQDENPVVHFF (aa 107–117) (Fig. 3A). Another prominent MBP peptide derived from N-terminal proteolysis is HGSKYLATASTMD (aa 11–24) (Fig. 3C), which is observed in multiple TBI CSF ultrafiltrate samples (Suppl. Fig. S4). This is followed by proteolysis of the center region counterpart with peptides such as KNIVTPRTPPPSQG (aa 117–130) or IVTPRTPPPSQG (aa 119–130) (Fig. 3B, C). In addition to the classic MBP, there is human Golli-MBP isoform 1 (accession # P02686-1) (304 aa, 34 K), which has a distinct N-terminal sequence aa 11–133 followed by the full sequence of the classic MBP Isoform 5 (accession # P02686-5, 171 aa; 18.5 K) (Suppl. Fig. S5). Thus, MBP proteolytic peptides found in classic MBP could potentially come from the Golli-MBP1. We have evidence that Golli-MBP-only peptides are present in human TBI CSF patients—a major peptide HAGKRELNAEKASTNSETNRGESEKKRNLGE (Suppl. Fig. S5) and a minor peptide NAWQDAHPADPGSRPHLIRLFSRDAPGREDNTFKDRPSESDE (Suppl. Fig. S6). Lastly, by using an anti-MBP antibody that targets the IVTPRTPPPSQG epitope, we identified strong MBP-BDP-8 K bands in most TBI CSF patients (24 h post-injury) when compared to controls (Fig. 3D). The median of MBP-BDP-8 K levels in TBI CSF retentate was significantly higher than their control counterparts (Fig. 3E).

In Vitro Purified Neurogranin, Vimentin, and Myelin Basic Protein Digestion Also Yielded Similar Proteolytic Peptides

As additional proof of principle, we also obtained purified human neurogranin, vimentin, and MBP proteins and subjected them to calpain-1 digestion, followed by ultrafiltration. The ultrafiltrate samples for NRGN with calpain-1 digestion indeed contained a cluster of peptides from residues 24 to 43 and 48 to 68. An example is 24–35: PGANAAAAKIQA. These match well with the human TBI CSF neurogranin peptide pattern (Suppl. Figure 7A, B). In contrast, we identified only a single peptide from caspase-6 digestion: aa 16–22 ILDIPLD (Suppl. Figure 7C, D). It becomes obvious, by adding the four preceding amino acids [(PDDD)ILDIPLD],

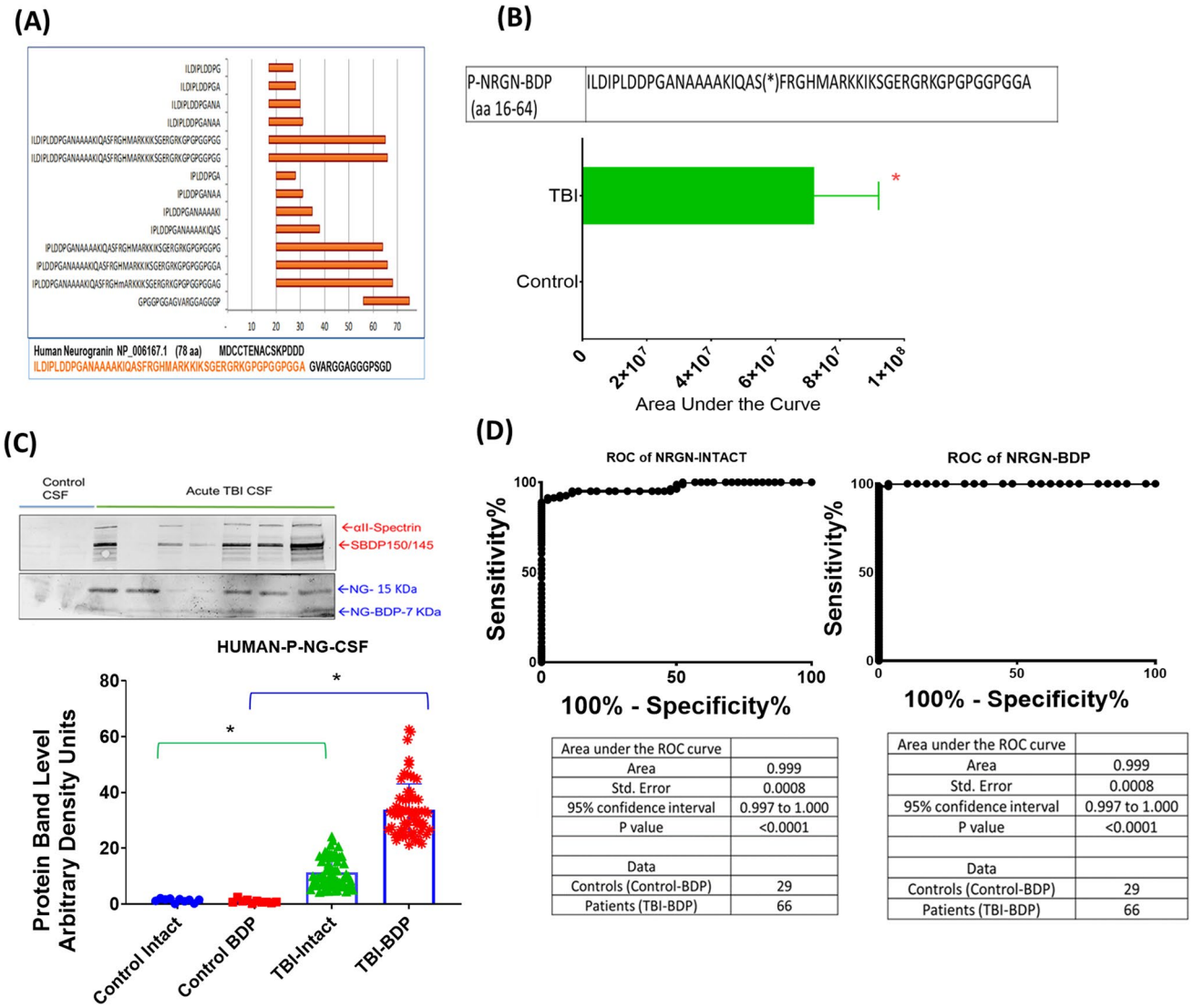

Area under the ROC curve	
Area	0.999
Std. Error	0.0008
95% confidence interval	0.997 to 1.000
P value	<0.0001
Data	
Controls (Control-BDP)	29
Patients (TBI-BDP)	66

Area under the ROC curve	
Area	0.999
Std. Error	0.0008
95% confidence interval	0.997 to 1.000
P value	<0.0001
Data	
Controls (Control-BDP)	29
Patients (TBI-BDP)	66

Fig. 1 P-Neurogranin proteolytic peptides and neurogranin-BDP characterization in CSF from human TBI ($N=10$) subjects. **A** Schematic representation of the NRGN peptides generated and released into human CSF samples after TBI. Duplicate peptides are not shown. None of the peptides shown was found in non-injured control CSF samples ($N=10$). **B** Mass spectrometry based label-free quantification of the unique phospho-NRGN peptide (aa 16–64) in TBI ($N=10$) vs. control CSF ($N=10$) samples (≤ 24 h). **C** Immunoblots of intact NRGN and NRGN-BDP (7 kDa) in human TBI CSF ($N=66$) samples vs. control CSF ($N=29$) using internal epitope antibody (EMD AB5620). Loading control β-actin (43 kDa) was not applied as brain proteins are expected to be unevenly released into biofluid (i.e., more in TBI samples, less in normal samples), and equal CSF volume was loaded to mimic the ELISA-based diagnostic test where biomarker levels are reported as pg or ng per mL. In addition, positive biomarker control was employed, and the blot was concurrently probed with II-spectrin antibody (MAb). The lower panel shows densitometric quantification of the intact and BDPs of the NRGN are shown as a bar/scattered plot with mean and SEM. An asterisk shows statistical significance over naïve p value <0.05, 2-tailed unpaired T test. **D** ROC curves of intact NRGN and P-NRGN-BDP comparing control CSF ($N=29$) vs. TBI CSF ($N=66$). Each ROC curve's, area under the curve, SEM, 95% confidence interval, and p value are shown under the curve, respectively

that cleavages generating the ILDIPLD peptide fulfill the XXXD requirement immediately at N-terminal for the amide bond cleavage for caspase-6. However, this peptide was not observed in TBI CSF ultrafiltrate samples. When the purified neurogranin was digested by calpain-1 and caspase-3 that were run on SDS-PAGE and stained with Coomassie blue R250, a distinct NRGN-BDP of 7 K was readily observed with calpain-1 but not with caspase-3 (Suppl. Figure 8A). In a second experiment, NRGN was digested with calpain-1, caspase-3, and caspase-6, and the retentate was probed with the anti-NRGN antibody. Calpain-1 digestion reduced intact NRGN levels significantly and 1/5 strength calpain-1 also yielded the signature NRGN-BDP of 7 K, while caspase-6

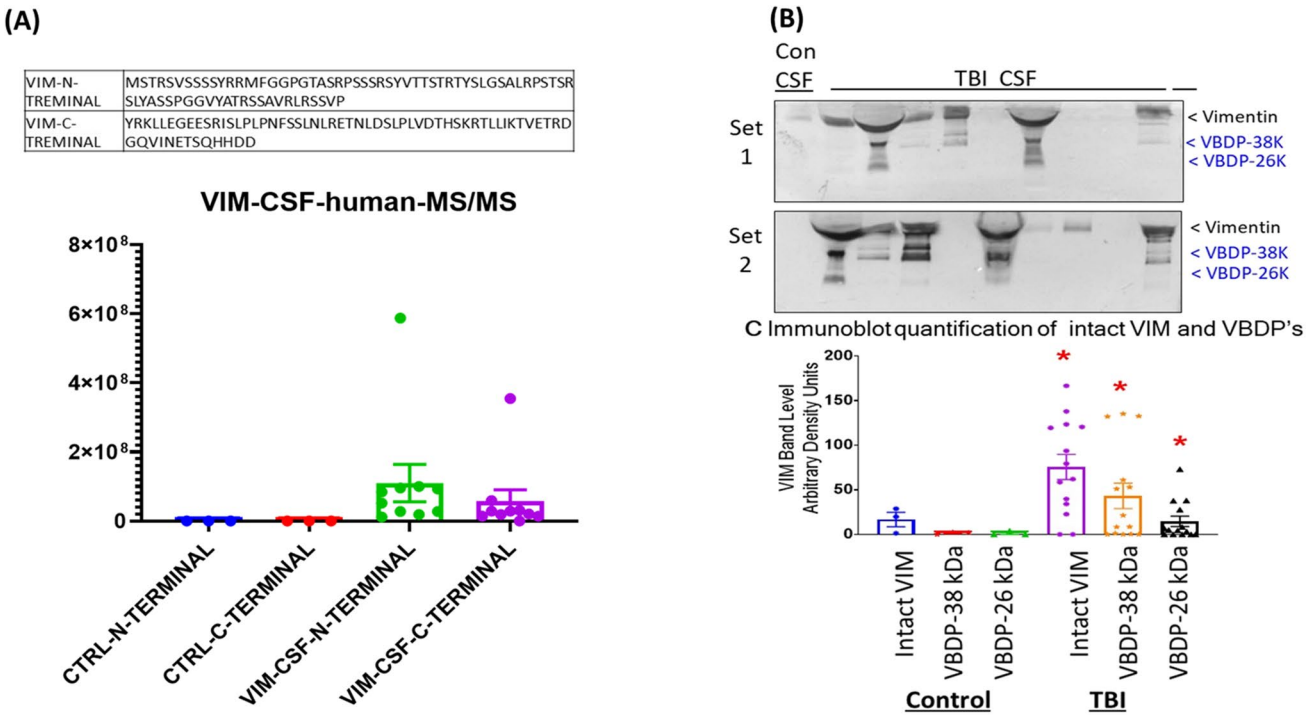

Fig. 2 Vimentin proteolytic peptides and vimentin-BDP characterization in CSF from human TBI ($N=10$) subjects. **A** Mass spectrometry based label-free quantification of VIM-N- and C-terminal proteolytic peptides (as indicated) in TBI ($N=10$) vs. control CSF ($N=10$) samples' mean and SEM are shown. An asterisk shows statistical significance over naïve p value <0.05, 2-tailed unpaired T test. **B** Human CSF profile of intact VIM breakdown to VIM BDP (VBDP) of 38 kDa and 26 kDa released after TBI ($N=30$) (≤ 24 h) as compared to controls ($N=20$). Western blot displaying the BDP (fragment) of VIM using anti-VIM internal epitope antibody (Abcam ab92547). Loading control β-actin was not applied (see explanation in the legend of Fig. 1). In addition, II-spectrin and SBDPs were shown as positive controls (data are not shown). **C** Densitometric quantification of the intact VIM and 38 kDa and 26 kDa VBDP are shown as a bar/scattered plot with mean and SEM. An asterisk shows statistical significance over naïve p value <0.05, 2-tailed unpaired T test)

produced a minor BDP of about 8 kDa, but not caspase-3 (Suppl. Figure 8B, C).

When vimentin protein was digested with calpain-1 and caspase-3, we found that both are capable of yielding numerous peptides. Calpain-1 digestion yields peptides in a major N-terminal cluster aa 1 to 65 with an example of MSTRSVSSSSYRRMFGGP (Suppl. Figure 9A). A less dominant cluster in the C-terminal was also observed—aa 405–466: LPLVDTHSKRTLLIKTVETRDGQVINETSQHHDD. Caspase-3 generates two peptides in the middle of the VIM molecule including (EAEE)WYKSKFADLSEAANRNND and (CEVD)ALKGTNESLERQMREMEENFAVEAANYQD (Suppl. Figure 9C). Again, these cleavages fit into the XXXD/E N-terminal to amide bond cleavage requirement for caspase-3. When purified vimentin protein is first subjected to calpain, it was found to be extensively degraded based on Coomassie blue-stained gel evidence (Suppl. Figure 10A). We further subjected VIM to calpain and caspase digestion and the ultrafiltration retentates were analyzed by immunoblot analysis, VIM is shown as a better substrate for calpain-1 than calpain-2, processing completely to VBDP of about 37 K–38 K, while calpain-2 only processes VIM partially to intermediate fragments of 40 K–44 K (Suppl. Figure 10B). Caspase-3, on the other hand, only partially degrade VIM to VBDP of 44–40 K, and a minor VBDP of 30 K, while VIM was partially degraded by caspase-6 to VBDP 44–40 K, 30 K, and 26 K caspase-6 (Suppl. Figure 10C).

Finally, for MBP, we used native human MBP containing isoforms 3 and 4 (21 K–18.5 K), as Golli-MBP was not commercially available. Since we have previously shown that MBP is vulnerable to calpain-1 but not caspase-3 [19, 31], thus, we focused on calpain-1 digestion and observed an N-terminal fragment at aa 34–44: RDTGILSIGR, and a cluster of fragments in the center region—aa 118–129: KNIVTPRTPPPSQGKGRGLSLS (Suppl. Figure 11 A, D). Again, a robust MBP peptide TPRTPPPSQGKGRGLSLS (aa 96–113) was found. Thus, the overall MBP proteolytic peptide pattern is highly similar to those found in TBI CSF (Fig. 4). On SDS-PAGE gel stained with Coomassie blue and/or anti-MBP antibody (SMI99 MAb)-probed immunoblot, MBP sample digestion showed major MBP-DBPs about 8–10 K (Suppl. Figure 11 C, E).

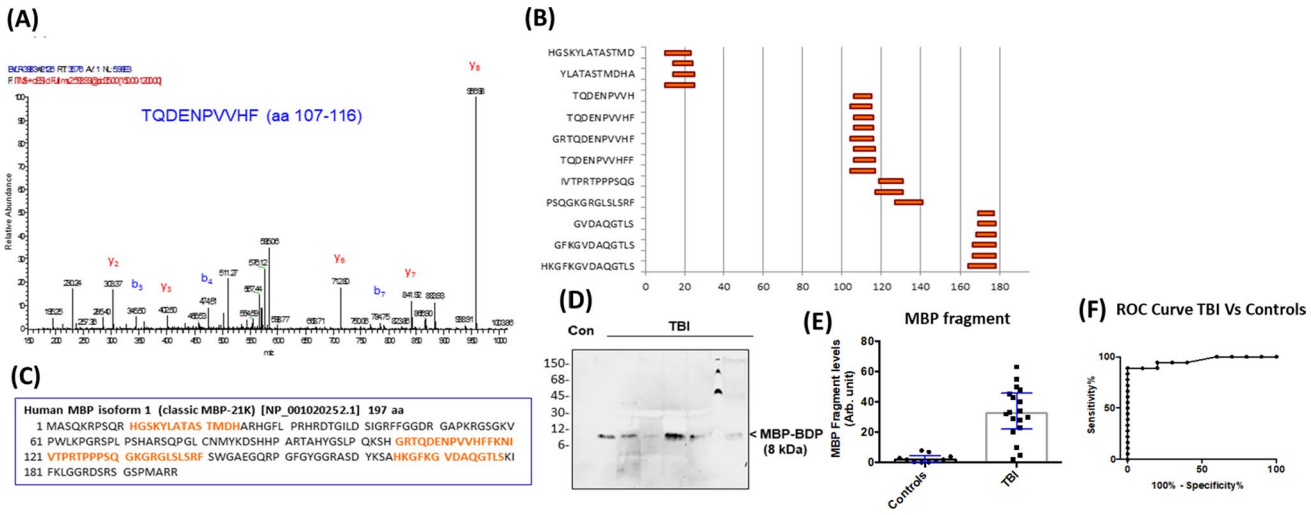

Fig. 3 Classic MBP proteolytic peptides and MBP-BDP identification in CSF from human TBI subjects. **A** MS/MS spectrum of the MBP peptide TQDENPVVHF (amino acid residues 107–116), based on classic human MBP isoform 3, 197 aa MBP-21.5 K charge of 2+, monoisotopic *m*/*z* 593.96, released in CSF samples in TBI subjects ($N=10$) (≤ 24 h). **B** Schematic representation for the MBP peptides generated and released into CSF samples. Duplicate peptides found are not shown. None of the peptides shown was found in non-injured control CSF samples ($N=10$). Residue # is shown on the *X*-axis. **C** Human MBP isoform 1 [accession # NP_001020252.1] amino acid sequence. Residues in orange show coverage by classic MBP peptides released. **D** Human CSF profile of MBP-fragment (BDP) of 8 kDa release after TBI (≤ 24 h) as compared to controls. Western blot displaying the BDP (fragment) of MBP using anti-MBP (SMI99 Mab). Loading control β-actin was not applied (see explanation in the legend of Fig. 1). Also, II-spectrin and SBDPs were examined as positive controls (see Fig. 1). **E** Densitometric quantification of the intact MBP and 8 kDa MBP-BDP are shown as a bar/scattered plot with mean and SEM. An asterisk shows statistical significance over naïve p value < 0.05, 2-tailed unpaired T test. **F** ROC curves of intact MBP comparing control CSF vs. TBI CSF. Each ROC curve's, area under the curve, SEM, and 95% confidence interval

MBP Targeted Peptide Quantification

For more quantitative validation of two TBI-produced proteolytic peptides, we used a heavy isotope to synthesize two peptides of MBP TQDENPVVHF (aa 107–116) and TQDENPVVHFF (aa 107–117). A heavy isotope-labeled peptide, TQDENPVVHFF and TQDENPVVHF have been synthesized to validate them against an independent set of pooled samples from a different cohort of subjects: healthy control CSF ($n=15$) independent set; CSF from TBI subjects was collected from the same patients within 6–12 h post-admission (acute $n=15$) or 96–120 h post-admission (subacute, $n=13$); two subjects do not have the subacute; Fig. 5A, B depicts light (native) and heavy peptide signals from both TQDENPVVHFF and TQDENPVVHF in each of the 3 pooled samples. Based on the ratio of the native light vs. heavy isotope-labeled peptide, we were able to quantify both MBP peptides and established that they were significantly elevated in individual non-pooled TBI CSF samples vs. non-pooled healthy control CSF samples (Fig. 6). TQDENPVVHFF has median concentrations of 1172.97 and 505.86 pg/mL in acute and subacute CSF as compared to 108.65 pg/mL in healthy controls. TQDENPVVHF concentrations were 669.30 and 703.71 pg/mL in acute and subacute TBI CSF, as compared to 260.71 pg/mL in the healthy control CSF. Acute and subacute TBI CSF levels for both peptides are significantly higher than control CSF (Fig. 6).

Discussion

The peptidome in a healthy brain represents an array of bioactive neuropeptides and also some levels of peptides usually derived from non-specific, intact protein truncation at the N- and C-terminals. The concept of peptidome as a possible source of biomarkers has been proposed for neurodegenerative diseases, such as Alzheimer's disease, schizophrenia, and other human diseases [27, 29, 41, 42]. This is the first systematic TBI-based proteolytic peptidome study. Our overall results showed that TBI not only produces truncated brain protein fragments but also simultaneously releases or sheds low molecular weight proteolytic peptides from the target proteins. Our results showed that diverse cell types, subcellular, and extracellular structures are vulnerable to the physical impact as well as the subsequent neurochemical imbalances. As a result, local over-activated proteolytic enzymes attack unique proteins from these cell types or subcellular or extracellular structures. This, in turn, results in the formation of large breakdown products and the release of a set of proteolytic

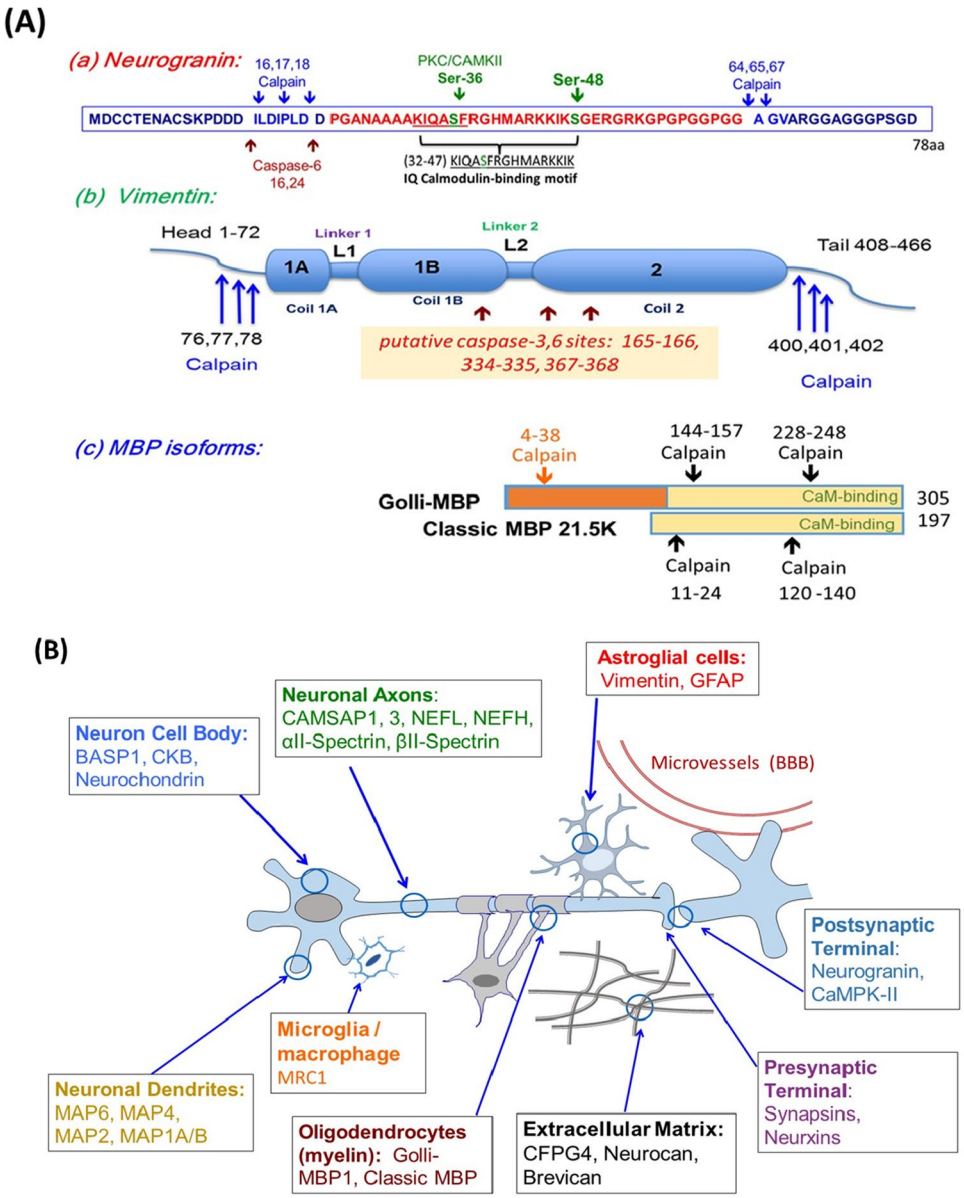

Fig. 4 Composite schematic summary of TBI proteolytic peptidome and proteolytic breakdown product formation. **A** Mapping major proteolytic sites of four brain proteins (neurogranin, vimentin and Golli-MBP, and classic MBP) vulnerable to TBI-induced proteolytic attack, yielding LMW peptides and protein-BDPs. Based on human sequences, (**a**) *Neurogranin*: major calpain-1, caspase-6 cleavage sites, PKC/CaMPKII phosphorylation site (Ser-36, 48), and calmodulin-binding motif (32–47) are shown. (**b**) *Vimentin*: head and tail, central coils and linker regions, major calpain-1, and putative caspase-3,6 cleavage sites are shown. (**c**) *MBP*: both Golli-MBP (305 aa) and classic MBP 21.5 K (197 aa) are shown. With major Golli-MBP isoform-specific and common calpain-1 cleavage sites, and calmodulin-binding motif present at the C-terminal (YKSAHKGFKGVDAQGTL-SKI FKLGGRDSRS GSP-MARR). **B** Graphic representation of TBI-vulnerable brain proteolytic targets in different cell types (neuron, astroglia, oligodendrocyte), subcellular compartments in neurons (axons, dendrites, cell body, pre- and post-synaptic terminals), and extracellular matrix, as derived from our overall data (see body for more details)

peptides into biofluids. We termed this as TBI proteolytic peptidome (Suppl. Figure 1).

Archived acute CSF samples from human TBI and control subjects were used. Peptidome analysis was conducted without added protease (such as trypsin) and directly subjected to nLC-MS/MS analysis and bioinformatic searches to identify the parent proteins. Thus, all peptides identified represented natively released peptides. We employed a high-throughput ultrafiltration method; thus, LMW peptide fractions (< 10 kDa) were collected in the ultrafiltrate, whereas HMW and larger intact protein and protein-BDPs were retained in the retentate. From the human TBI CSF ultrafiltrate samples, based on the origin of proteolytic peptide release, we identified widespread proteolysis occurring in neurons, astrocytes, oligodendrocytes, and microglia/macrophage cells and extracellular matrix, resulting in brain-resident protein truncations and the concurrent release of a pool of distinct LMW proteolytic peptides (Suppl. Table 1). Distinct proteolytic peptides are derived from resident proteins in major neuronal subcellular compartments—cell body, axons, dendrites, presynaptic terminal, and post-synaptic density (Table 2).

To further gain insight into the generation and patterns of such proteolytic peptides, we focused on a subset of proteins (neurogranin, vimentin, Golli-MBP1, and MBP4) with prominent peptides displaced in the peptidome dataset. Neurogranin is an abundant post-synaptic protein. It has been found elevated in CSF samples from Alzheimer's disease subjects [37]. Our finding focuses on the core predominant NRGN phosphorylated peptide, identified (aa 16–64),

phosphorylated at Ser-36 and Ser-48 (data not shown) which showed an elevation in the CSF of traumatic brain injury patients. Thus, this report is the first to identify that neurogranin is processed by protease(s) into proteolytic peptides and then released into biofluid. The phosphorylation of neurogranin at Ser-36/48 has not been previously described. This truncated core region of NRGN also contains the IQ calmodulin-binding motif (aa 32–47) (Fig. 4A, (a),) [43]. Phosphorylation of the calmodulin-binding region in other calmodulin-binding proteins are known to interfering with their functions [44]. Since intact NRGN's calculated molecular weight is only 7.62 kDa, thus, we suspected that the observed NRGN-BDP actual MW is likely about 5 kDa—that put it in the same size range as the core peptides we observed by MS/MS. We also noted that the pattern of NRGN cleavage is more consistent with those generated by calpain-1 rather than caspase-3/-6 (Suppl. Figure 8). Thus, this truncated and phosphorylated NRGN fragment might have a pathophysiologic role in synaptic dysfunction after TBI and potentially be a point of care diagnostic tool.

Another been previously undescribed potential biomarker for TBI is vimentin (466 amino acids)—which is an astroglial-dominant intermediate filament protein. We observed that the majority of the peptides were derived from the shedding of the N-terminal (first 90–100 residues) or C-terminal (last 50–60 residues) region in human TBI (Suppl. Figure 3). Such shedding and truncation from both N- and C-terminals are further confirmed by TBI CSF retentate samples by immunoblotting analysis (showing the formation of major core-spanning BDP of 38 kDa) (Fig. 3B). From the general structural model of vimentin, the N- and C-terminal shedding is consistent with the clipping of the head and tail domains while sparing the center core (Fig. 4A, (b)). In parallel, we identified three potential internal caspase cleavage sites (human VIM aa: 165–166, 334–335, 367–368) (Suppl. Figure 10). However, these were not observed in human TBI samples; thus, caspase involvement in vimentin proteolysis is likely a minor event in TBI.

A third novel pathological biomarker target identified by our systemic proteolytic peptidomics analysis is Golli-MBP. There are two major subclasses of MBP—the classic MBP (human isoform 3–12), which is often observed in myelin sheath, and the second group is the Golli-MBP that has a distinct N-terminal of 120 aa (Suppl. Figure 10). Golli-MBP is thought to be more prominent in brain development as well as a range of other functions in neuronal and non-neuronal cells. Rather unexpectedly, we found the release of Golli-MBP-specific N-terminal peptides in the human dataset (e.g., HAGKRELNAEKASTNSETNRGESEKKRNLGE, aa 4–34) (Supp. Figure 11). These data suggest that Golli-MBP might have more prominent structural and functional roles in the mature brain than originally thought. Lastly, a Golli-MBP/classic MBP-common C-terminal short peptide region was also observed in the human TBI CSF ultrafiltrate (HKGFKGVDAQGTLS) (Fig. 3). It has been reported that classical MBP is subjected to proteolysis [25], but this is the first report to identify the processing of Golli-MBP after TBI and that such Golli-MBP peptides are released into biofluid.

Another novel insight of our peptidomics data was the vulnerability of extracellular matrix structural proteins, as evidenced by the presence of proteolytic peptides released from chondroitin sulfate proteoglycan 4 (CSPG4) as well as neurocan core protein of CSPG3 and brevican (CSPG7) in human TBI samples (Table 2). CPG4 is made up of proteoglycan and covalently linked chondroitin sulfate (sulfated glycosaminoglycan) at the C-terminal. It is also called neuron-glial antigen 2 (NG2). In addition to interacting with other major extracellular scaffold proteins (such as tenascin), CSPG4 itself is also released by the action of MMP or other transmembrane membrane-bound MMP (TM-MMP) into the extracellular matrix itself. CSPG4 is enriched in the brain and thought to play key roles in neural development and glial scar formation and neural repair after brain injury [45, 46]. The breakdown of the proteoglycan component and the release of proteolytic peptides from such CSPG3, CSPG4, and CSPG7 could have significant extracellular scaffold destabilizing effects (Fig. 4B). Possible protease candidates are MMPs (e.g., MMP-2, MMP-9), which are already shown to be activated following TBI and other forms of brain injury [46]. This area requires further investigation.

Importantly, all TBI CSF samples have evidence of proteolytic peptidome. Based on our data, we proposed NGRN, VIM, and MBP proteolytic peptide signature could be used to study TBI. Suppl. Table 4 lists such a panel. For classic tryptic peptides, one can use multiple reaction monitoring (MRM)/parallel reaction monitoring (PRM) methods in MS/MS and the synaptic tryptic peptides as internal standards for the quantification of natively generated peptides [1]. Importantly for our TBI-induced proteolytic peptides, we also attempted validation by synthesizing two dominant MBP peptides (TQDENPVVHF (aa 107–116) and TQDENPVVHFF (aa 107–117)) using heavy isotope-labeled peptides as quantification standard in targeted MS/MS quantification using $N = 10$ TBI (acute 24 h and subacute 72 h) samples and $N = 10$ control samples—with both of them showing strong TBI differentiation (Fig. 5).

One limitation of our study is that we have not developed an optimized quantification method of key peptides for the NRGN and VIM, especially for blood-based detection. We believe that ultimately, antibody-based competitive enzyme-linked immunosorbent assay (ELISA) will be the method of choice for their quantification. For example, one could produce an antibody that targets the peptide epitope region of interest. We could develop a competitive ELISA method that is combined with ultrafiltration-based LMW peptide enrichment for high-precision quantification. Once this type

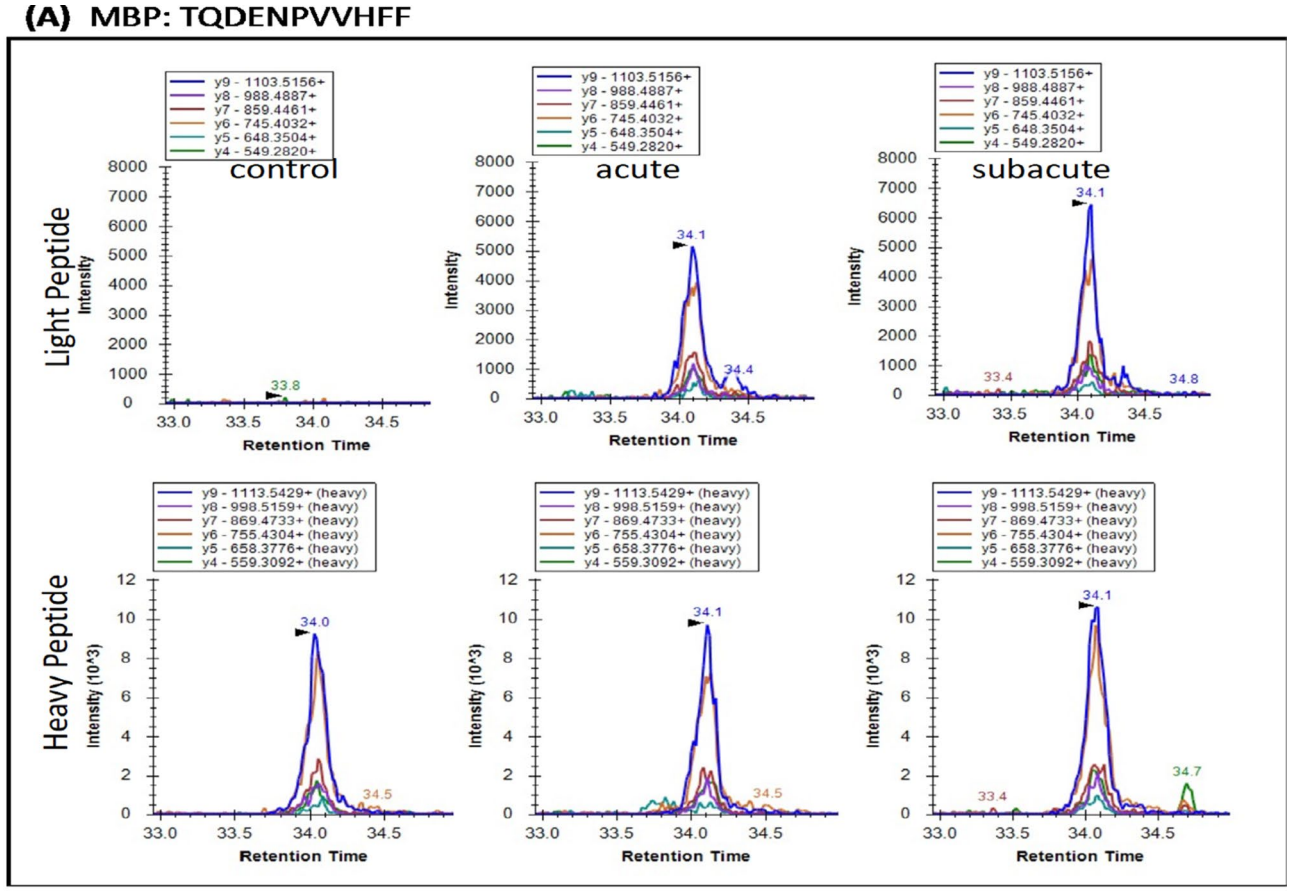
(A) MBP: TQDENPVVHFF
Light Peptide
Heavy Peptide
control
acute
subacute
y9 - 1103.5156+
y8 - 988.4887+
y7 - 859.4461+
y6 - 745.4032+
y5 - 648.3504+
y4 - 549.2820+
y9 - 1113.5429+ (heavy)
y8 - 998.5159+ (heavy)
y7 - 869.4733+ (heavy)
y6 - 755.4304+ (heavy)
y5 - 658.3776+ (heavy)
y4 - 559.3092+ (heavy)
Intensity
Intensity (10^3)
Retention Time
33.8
34.1
34.4
33.4
34.8
34.0
34.5
34.7

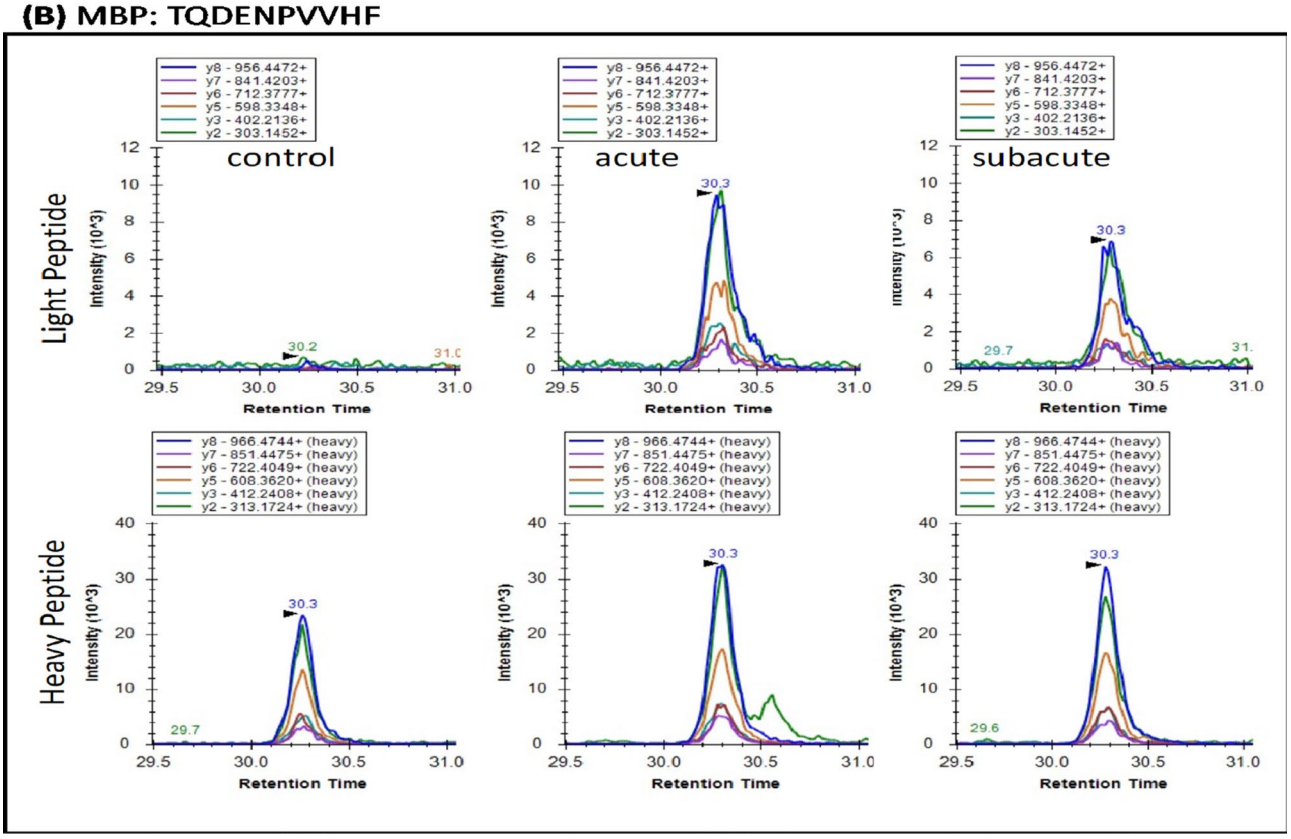
(B) MBP: TQDENPVVHF
Light Peptide
Heavy Peptide
control
acute
subacute
y8 - 956.4472+
y7 - 841.4203+
y6 - 712.3777+
y5 - 598.3348+
y3 - 402.2136+
y2 - 303.1452+
y8 - 966.4744+ (heavy)
y7 - 851.4475+ (heavy)
y6 - 722.4049+ (heavy)
y5 - 608.3620+ (heavy)
y3 - 412.2408+ (heavy)
y2 - 313.1724+ (heavy)
Intensity
Intensity (10^3)
Retention Time
30.2
31.0
30.3
29.7
31.
29.6

◂**Fig. 5** Targeted LC/MS/MS extracted ion chromatograms for light and heavy versions of MBP peptides in pooled control CSF and in acute and subacute time collected TBI CSF: **A** TQDENPVVHFF and **B** TQDENPVVHF. Heavy peptides were spiked in at 20 fmol/50 µL of pooled CSF before ultrafiltration with a 10 kDa membrane

of method is developed, we can address if these peptides are also readily detectable in serum biosamples. In addition, thus far, we have focused on severe TBI subjects. With such a quantification method, we can examine if the proteolytic peptidome is also produced in mild TBI in human. Another limitation is that the current study was intended for proteolytic peptidome discovery; thus, only relatively small sample sizes ($N=66$ TBI, $N=29$ controls) were used. For future quantitative proteolytic peptide biomarker verification studies, a large study cohort should be used. Another limitation is that non-CNS injury control CSF would have been the ideal comparison of the TBI CSF samples. However, CSF collection from such patients would not be medically indicated and is difficult to justify in an IRB protocol. Thus, this is beyond the scope of our study. In the future, such a control study should be done as further validation of our results. Lastly, in the future, it will be important to examine if one or more of these proteolytic peptide marker levels in biofluid (CSF or blood) will correlate with patient outcomes.

In summary, our study reveals widespread and robust intracellular and extracellular proteolysis after TBI (Fig. 4B). Due to the destructive nature of proteolysis, these findings imply that future therapeutic strategies might be placed on the suppression of brain proteolysis as a target. The native endogenous NRGN peptide (Fig. 1B) discovered in human TBI CSF represents a potential tool for monitoring TBI progression.

Their biofluid levels might reflect the status of TBI pathologies such as synaptic dysfunction and might be useful in tracking severity, disease progress, or recovery. Secondly, since proteolytic peptides are relatively small in size, they might be readily permeable to the brain-blood barrier and become accessible in circulating blood. Thus, monitoring a subset of this endogenously generated brain-resident protein breakdown products and the accompanied proteolytic peptides in biofluid might have fruitful TBI diagnostic biomarker potentials. Lastly, this study demonstrates remarkable widespread proteolytic proteome release from human TBI. Thus, it argues that a well-designed concurrent diagnostic study is a viable and powerful approach in gaining insights into the pathogenesis of TBI and potentially other neurological disorders.

Supplementary Information The online version contains supplementary material available at https://doi.org/10.1007/s12035-021-02600-w.

Acknowledgements We thank Drs. Alejandro Cohen and Benjamin W. Smith, for their constructive comments, critical reading, and assistance.

Author Contribution
- Substantial contribution to the concept, design of the article, acquisition, analysis, and interpretation of data for the article: GAS, KKWW.
- Drafted the article and revised it critically for important intellectual content: GAS, KKWW, RAY, NLG, JB
- Review: GAS, CR, WEH
- Experimental: GAS, SEA

Funding Departmental funding from the Department of Chemistry, Psychiatry and Emergency Medicine, UF, is gratefully recognized. This study is also supported in part by U.S. DOD TED Seed Project TED1506 (DOD W81XWH-14–2-0176) (KKW); NIH R21NS085455-01 (KKW); VA I01 RX001859-02 Merit Award (KKW); Florida State/McKnight Brain Institute BSCIRT Fund (#110587) (KKW); NIH 1U01 NS086090-01 (KKW, PI Geoff T Manley (GTM)), DOD Grant W81XWH-14–2-0176 (KKW, GTM); and NIH-NINDS (#P01-NS38660) (CSR).

Data Availability Data are available for the reader who makes a direct request to the corresponding authors.

Declarations

Ethics Approval and Consent to Participate Ethics approval was obtained for this research involving human subjects. Patients have given informed consent for continuing use of archived CSF samples used in this study (Baylor College of Medicine IRB protocol. Protocol Number: H-44131 and H-31722).

Consent for Publication The corresponding author grants consent on behalf of all authors.

Competing Interests Kevin K. W. Wang and William E. Haskins are shareholders of Gryphon Bio, Inc. The other authors declare no competing interests.

References

1. Sarkis GA, Mangaonkar MD, Moghieb A et al (2017) The application of proteomics to traumatic brain and spinal cord injuries. Curr Neurol Neurosci Rep 17:23. https://doi.org/10.1007/s11910-017-0736-z
2. Rusnak M (2013) Traumatic brain injury: giving voice to a silent epidemic. Nat Rev Neurol 9:186–187. https://doi.org/10.1038/nrneurol.2013.38
3. Haring RS, Narang K, Canner JK et al (2015) Traumatic brain injury in the elderly: morbidity and mortality trends and risk factors. J Surg Res 195:1–9. https://doi.org/10.1016/j.jss.2015.01.017
4. Levin HS, Diaz-Arrastia RR (2015) Diagnosis, prognosis, and clinical management of mild traumatic brain injury. Lancet Neurol 14:506–517. https://doi.org/10.1016/S1474-4422(15)00002-2
5. Zhang Z, Moghieb A, Kevin K, Wang W (2020) In Biomarkers of brain injury and neurological disorders, K. K. W. Wang, Z. Zhang, F. H. Kobeissy, Eds. (CRC Press), pp. 652
6. Centers for Disease (2013) Control, Prevention, CDC grand rounds: reducing severe traumatic brain injury in the United States MMWR Morb. Mortal Wkly Rep 62:549–552

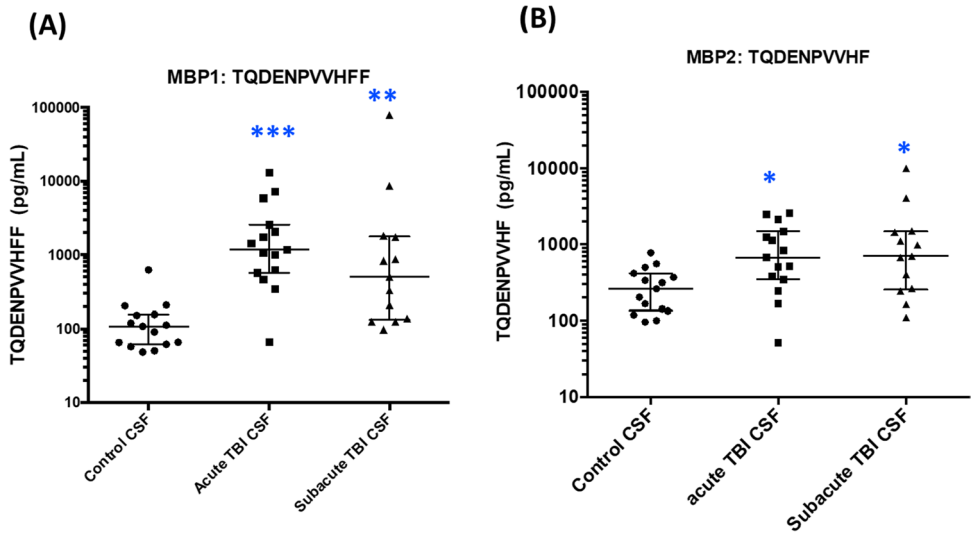

Fig. 6 Selected MBP proteolytic peptide quantification in human TBI CSF samples vs. control CSF samples ($N = 13–15$ independent set). **A** MBP peptide TQDENPVVHFF. **B** MBP peptide TQDENPVVHF. Acute TBI CSF samples were collected within 6–12 h post-admission. Subacute TBI CSF samples were collected 96–120 h post-admission. Shown are scattered plots and bars of median and 95% confidence intervals. By the Kruskal–Wallis test for the group, p values < 0.05 for both peptides. With Dunn's comparison test, acute TBI are significantly higher than control CSF for both peptides ($*p < 0.05$; $**p < 0.01$, $***p < 0.001$)

7. DOD-DVBIC, DVBIC Worldwide-TBI 2000–2013 Report, DOD Report, 1–5 (2014).
8. McMahon P, Hricik A, Yue JK et al (2014) Symptomatology and functional outcome in mild traumatic brain injury: results from the prospective TRACK-TBI study. J Neurotrauma 31:26–33. https://doi.org/10.1089/neu.2013.2984
9. Wang KK (2000) Calpain and caspase: can you tell the difference? Trends Neurosci 23:20–26
10. Siesjö BK, Bengtsson F, Grampp W, Theander S (1989) Calcium, excitotoxins, and neuronal death in the brain. Ann N Y Acad Sci 568:234–251. https://doi.org/10.1111/j.1749-6632.1989.tb12513.x
11. Wang null (2000) Calpain and caspase: can you tell the difference?, by kevin K.W. WangVol. 23, pp. 20–26. Trends Neurosci 23:59. https://doi.org/10.1016/s0166-2236(99)01479-4
12. Pineda JA, Wang KK, Hayes RL (2004) Biomarkers of proteolytic damage following traumatic brain injury. Brain Pathol Zurich Switz 14:202–209
13. Pike BR, Flint J, Dutta S et al (2001) Accumulation of non-erythroid alpha II-spectrin and calpain-cleaved alpha II-spectrin breakdown products in cerebrospinal fluid after traumatic brain injury in rats. J Neurochem 78:1297–1306. https://doi.org/10.1046/j.1471-4159.2001.00510.x
14. Siman R, Toraskar N, Dang A et al (2009) A panel of neuron-enriched proteins as markers for traumatic brain injury in humans. J Neurotrauma 26:1867–1877. https://doi.org/10.1089/neu.2009.0882
15. Shaw G, Yang C, Zhang L et al (2004) Characterization of the bovine neurofilament NF-M protein and cDNA sequence, and identification of in vitro and in vivo calpain cleavage sites. Biochem Biophys Res Commun 325:619–625. https://doi.org/10.1016/j.bbrc.2004.09.223
16. Zoltewicz JS, Mondello S, Yang B et al (2013) Biomarkers track damage after graded injury severity in a rat model of penetrating brain injury. J Neurotrauma 30:1161–1169. https://doi.org/10.1089/neu.2012.2762
17. Zhang Z, Zoltewicz JS, Mondello S et al (2014) Human traumatic brain injury induces autoantibody response against glial fibrillary acidic protein and its breakdown products. PLoS ONE 9:e92698. https://doi.org/10.1371/journal.pone.0092698
18. Chen M-H, Hagemann TL, Quinlan RA et al (2013) Caspase cleavage of GFAP produces an assembly-compromised proteolytic fragment that promotes filament aggregation. ASN Neuro 5:e00125. https://doi.org/10.1042/AN20130032
19. Liu MC, Akle V, Zheng W et al (2006) Extensive degradation of myelin basic protein isoforms by calpain following traumatic brain injury. J Neurochem 98:700–712. https://doi.org/10.1111/j.1471-4159.2006.03882.x
20. Ottens AK, Kobeissy FH, Wolper RA et al (2005) A multidimensional differential proteomic platform using dual-phase ion-exchange chromatography−polyacrylamide gel electrophoresis/reversed-phase liquid chromatography tandem mass spectrometry. Anal Chem 77:4836–4845. https://doi.org/10.1021/ac050478r
21. Luo C-L, Chen X-P, Yang R et al (2010) Cathepsin B contributes to traumatic brain injury-induced cell death through a mitochondria-mediated apoptotic pathway. J Neurosci Res 88:2847–2858. https://doi.org/10.1002/jnr.22453
22. Zhang Z, Ottens AK, Sadasivan S et al (2007) Calpain-mediated collapsin response mediator protein-1, -2, and -4 proteolysis after neurotoxic and traumatic brain injury. J Neurotrauma 24:460–472. https://doi.org/10.1089/neu.2006.0078
23. Shibayama M, Kuchiwaki H, Inao S et al (1997) Induction of matrix metalloproteinases following brain injury in rats. Acta Neurochir Suppl 70:220–221
24. Yamashima T (2000) Implication of cysteine proteases calpain, cathepsin and caspase in ischemic neuronal death of primates. Prog Neurobiol 62:273–295
25. Chen C-D, Tung TY, Liang J et al (2014) Identification of cleavage sites leading to the shed form of the anti-aging protein klotho. Biochemistry 53:5579–5587. https://doi.org/10.1021/bi500409n
26. Conant K, Allen M, Lim ST (2015) Activity dependent CAM cleavage and neurotransmission. Front Cell Neurosci 9https://doi.org/10.3389/fncel.2015.00305
27. Svensson M, Skvld K, Nilsson A et al (2007) Neuropeptidomics: MS applied to the discovery of novel peptides from the brain. Anal Chem 79:14–21. https://doi.org/10.1021/ac071856q

28. Fricker LD (2010) Analysis of mouse brain peptides using mass spectrometry-based peptidomics: implications for novel functions ranging from non-classical neuropeptides to microproteins. Mol Biosyst 6:1355–1365. https://doi.org/10.1039/c003317k
29. Harauz G, Boggs JM (2013) Myelin management by the 18.5–kDa and 21.5–kDa classic myelin basic protein isoforms. J Neurochem 125:334–361. https://doi.org/10.1111/jnc.12195
30. Liu MC, Kobeissy F, Zheng W et al (2011) Dual vulnerability of tau to calpains and caspase-3 proteolysis under neurotoxic and neurodegenerative conditions. ASN Neuro 3:e00051. https://doi.org/10.1042/AN20100012
31. Ottens AK, Golden EC, Bustamante L et al (2008) Proteolysis of multiple myelin basic protein isoforms after neurotrauma: characterization by mass spectrometry. J Neurochem 104:1404–1414. https://doi.org/10.1111/j.1471-4159.2007.05086.x
32. Yang Z, Lin F, Robertson CS, Wang KKW (2014) Dual vulnerability of TDP-43 to calpain and caspase-3 proteolysis after neurotoxic conditions and traumatic brain injury. J Cereb Blood Flow Metab Off J Int Soc Cereb Blood Flow Metab 34:1444–1452. https://doi.org/10.1038/jcbfm.2014.105
33. Robertson CS, Hannay HJ, Yamal J-M et al (2014) Effect of erythropoietin and transfusion threshold on neurological recovery after traumatic brain injury: a randomized clinical trial. JAMA 312:36–47. https://doi.org/10.1001/jama.2014.6490
34. Díez-Guerra FJ (2010) Neurogranin, a link between calcium/calmodulin and protein kinase C signaling in synaptic plasticity. IUBMB Life 62:597–606. https://doi.org/10.1002/iub.357
35. Neuner-Jehle M, Denizot J-P, Mallet J (1996) Neurogranin is locally concentrated in rat cortical and hippocampal neurons. Brain Res 733:149–154. https://doi.org/10.1016/0006-8993(96)00786-X
36. Slemmon JR, Feng B, Erhardt JA (2000) Small proteins that modulate calmodulin-dependent signal transduction: effects of PEP-19, neuromodulin, and neurogranin on enzyme activation and cellular homeostasis. Mol Neurobiol 22:99–113. https://doi.org/10.1385/MN:22:1-3:099
37. De Vos A, Jacobs D, Struyfs H et al (2015) C-terminal neurogranin is increased in cerebrospinal fluid but unchanged in plasma in Alzheimer's disease. Alzheimers Dement J Alzheimers Assoc 11:1461–1469. https://doi.org/10.1016/j.jalz.2015.05.012
38. Schiffer D, Giordana MT, Migheli A et al (1986) Glial fibrillary acidic protein and vimentin in the experimental glial reaction of the rat brain. Brain Res 374:110–118. https://doi.org/10.1016/0006-8993(86)90399-9
39. Ekmark-Lewén S, Lewén A, Israelsson C et al (2010) Vimentin and GFAP responses in astrocytes after contusion trauma to the murine brain. Restor Neurol Neurosci 28:311–321. https://doi.org/10.3233/RNN-2010-0529
40. Pekny M, Pekna M, Messing A et al (2016) Astrocytes: a central element in neurological diseases. Acta Neuropathol (Berl) 131:323–345. https://doi.org/10.1007/s00401-015-1513-1
41. Wijte D, McDonnell LA, Balog CIA et al (2012) A novel peptidomics approach to detect markers of Alzheimer's disease in cerebrospinal fluid. Methods San Diego Calif 56:500–507. https://doi.org/10.1016/j.ymeth.2012.03.018
42. Cafe-Mendes CC, Ferro ES, Britto LRG, Martins-de-Souza D (2014) Using mass spectrometry-based peptidomics to understand the brain and disorders such as Parkinson's disease and schizophrenia. Curr Top Med Chem 14:369–381
43. Hoffman L, Chandrasekar A, Wang X et al (2014) Neurogranin alters the structure and calcium binding properties of calmodulin. J Biol Chem 289:14644–14655. https://doi.org/10.1074/jbc.M114.560656
44. Browne GJ, Proud CG (2004) A novel mTOR-regulated phosphorylation site in elongation factor 2 kinase modulates the activity of the kinase and its binding to calmodulin. Mol Cell Biol 24:2986–2997. https://doi.org/10.1128/mcb.24.7.2986-2997.2004
45. Aguirre A, Dupree JL, Mangin JM, Gallo V (2007) A functional role for EGFR signaling in myelination and remyelination. Nat Neurosci 10:990–1002. https://doi.org/10.1038/nn1938
46. Schäfer MKE, Tegeder I (2018) NG2/CSPG4 and progranulin in the posttraumatic glial scar. Matrix Biol J Int Soc Matrix Biol 68–69:571–588. https://doi.org/10.1016/j.matbio.2017.10.002